Vascular normalizing doses of antiangiogenic treatment reprogram the immunosuppressive tumor microenvironment and enhance immunotherapy

Vascular normalizing doses of antiangiogenic treatment reprogram the immunosuppressive tumor microenvironment and enhance immunotherapy

Yuhui Huang[a], Jianping Yuan[b], Elda Righi[b], Walid S. Kamoun[a], Marek Ancukiewicz[a], Jean Nezivar[b], Michael Santosuosso[b], John D. Martin[a], Margaret R. Martin[a], Fabrizio Vianello[b], Pierre Leblanc[b], Lance L. Munn[a], Peigen Huang[a], Dan G. Duda[a], Dai Fukumura[a], Rakesh K. Jain[a,1], and Mark C. Poznansky[b]

[a]Edwin L. Steele Laboratory of Tumor Biology, Department of Radiation Oncology and [b]Vaccine and Immunotherapy Center, Infectious Diseases Medicine, Massachusetts General Hospital and Harvard Medical School, Boston, MA 02114

Contributed by Rakesh K. Jain, September 8, 2012 (sent for review July 16, 2012)

The recent approval of a prostate cancer vaccine has renewed hope for anticancer immunotherapies. However, the immunosuppressive tumor microenvironment may limit the effectiveness of current immunotherapies. Antiangiogenic agents have the potential to modulate the tumor microenvironment and improve immunotherapy, but they often are used at high doses in the clinic to prune tumor vessels and paradoxically may compromise various therapies. Here, we demonstrate that targeting tumor vasculature with lower vascular-normalizing doses, but not high antivascular/antiangiogenic doses, of an anti-VEGF receptor 2 (VEGFR2) antibody results in a more homogeneous distribution of functional tumor vessels. Furthermore, lower doses are superior to the high doses in polarizing tumor-associated macrophages from an immune inhibitory M2-like phenotype toward an immune stimulatory M1-like phenotype and in facilitating $CD4^+$ and $CD8^+$ T-cell tumor infiltration. Based on this mechanism, scheduling lower-dose anti-VEGFR2 therapy with T-cell activation induced by a whole cancer cell vaccine therapy enhanced anticancer efficacy in a $CD8^+$ T-cell–dependent manner in both immune-tolerant and immunogenic murine breast cancer models. These findings indicate that vascular-normalizing lower doses of anti-VEGFR2 antibody can reprogram the tumor microenvironment away from immunosuppression toward potentiation of cancer vaccine therapies. Given that the combinations of high doses of bevacizumab with chemotherapy have not improved overall survival of breast cancer patients, our study suggests a strategy to use antiangiogenic agents in breast cancer more effectively with active immunotherapy and potentially other anticancer therapies.

vascular normalization | hypoxia | myeloid-derived suppressor cell | tumor tissue vaccine

After decades of research on harnessing the power of the immune system to fight cancer, the US Food and Drug Administration approved the first cancer vaccine (Provenge) to treat advanced prostate cancer in 2010 (1). However, tumor control by vaccination alone is minimal, and survival benefits remain modest. Thus, new approaches that improve the clinical benefits of anticancer vaccines are urgently needed.

The induction of high numbers of tumor-specific cytotoxic T lymphocytes is a prerequisite for successful cancer immunotherapy. Unfortunately, the presence of a high number of tumor antigen-specific cytotoxic T cells in peripheral immune organs often is not associated with clinical benefit (2, 3). Thus, other factors are likely involved in this poor clinical outcome. Among these, the tumor microenvironment is now considered a key player (4–8).

Emerging data indicate that abnormal tumor vasculature, resulting from the prevalence of pro- versus antiangiogenic signals, fosters an immunosuppressive tumor microenvironment that enables the tumor to evade host immunosurveillance (4, 6, 9). Proangiogenic factors not only suppress the function of various immune cells (10) but also diminish leukocyte–endothelial interactions and hinder the infiltration of immune effector cells into the tumor parenchyma (11). Clinical studies consistently support the view that malignant tumors are nonpermissive to T effector cell accumulation (3, 7, 12). In contrast, solid tumors usually are infiltrated with abundant immune suppressors, such as tumor-associated macrophages (TAMs), myeloid-derived suppressor cells (MDSCs), and regulatory T cells (Tregs) (13–15). Importantly, TAM and Treg accumulation within tumors correlates with poor prognosis (12–14, 16). Within breast cancer lesions, TAMs represent the dominant myeloid cell population and usually have an immunosuppressive M2-like phenotype associated with the hypoxic tumor microenvironment (14, 17, 18).

These immune-evasion mechanisms could be altered by antiangiogenic treatment. Rationally scheduled antiangiogenic treatment can transiently normalize tumor vessels, improve vessel perfusion, decrease hypoxia, and enhance cytotoxic therapies (4, 19–21). In genetic studies, vascular normalization by deletion of *Rgs5* increased T-cell infiltration into tumors and substantially improved survival after adoptive T-cell transfer in mice (9). Several preclinical studies have suggested that antiangiogenic therapy could increase tumor-infiltrating T cells (22–25). However, no antiangiogenic agent has been shown to improve breast cancer vaccine therapy in a clinically relevant model of immune-tolerant breast cancer (23). Here, we evaluate the effects of treatment with different doses of an anti-VEGF receptor 2 (VEGFR2) antibody (DC101) and establish a combinational regimen that synchronizes T-cell activation with breast cancer vascular normalization. In models of both immune-tolerant and immunogenic breast cancer, we show that lower doses, but not high dose, of DC101 can reprogram the immunosuppressive tumor microenvironment in a manner that augments anticancer vaccine therapy.

Results

Lower Doses of Anti-VEGFR2 Antibody Treatment Enhance Vaccine Therapy in a Model of MCaP0008 Breast Cancer. To test the dose-dependent effect of antiangiogenic treatment on cancer vaccine therapy in a clinically relevant breast cancer model, we vaccinated mice bearing orthotopic MCaP0008 breast cancer with a mitomycin C-pretreated MCaP0008 cancer cell vaccine, following different doses of DC101 treatment (Fig. 1*A*). Although vaccination stimu-

Author contributions: Y.H., J.Y., E.R., M.S., F.V., D.G.D., D.F., R.K.J., and M.C.P. designed research; Y.H., J.Y., E.R., J.N., M.S., and P.L. performed research; Y.H., W.S.K., J.D.M., M.R.M., L.L.M., P.H., D.G.D., D.F., R.K.J., and M.C.P. contributed new reagents/analytic tools; Y.H., J.Y., E.R., W.S.K., M.A., M.S., J.D.M., F.V., D.G.D., D.F., R.K.J., and M.C.P. analyzed data; and Y.H., D.G.D., D.F., R.K.J., and M.C.P. wrote the paper.

Conflict of interest statement: R.K.J. received research grants from Dyax, MedImmune, and Roche; consultant fees from Dyax, Enlight, Noxxon, and SynDevRx; owns equity in Enlight, SynDevRx, and XTuit; and serves on the Board of Directors of XTuit and Boards of Trustees of H&Q Healthcare Investors and H&Q Life Sciences Investors. M.C.P. serves as a scientific adviser to Evaxion-Biotech and owns equity in Celtaxsys. No reagents or funding from these companies was used in this study. Therefore, there is no significant financial or other competing interest in the work.

Freely available online through the PNAS open access option.

[1]To whom correspondence should be addressed. E-mail: jain@steele.mgh.harvard.edu.

This article contains supporting information online at www.pnas.org/lookup/suppl/doi:10.1073/pnas.1215397109/-/DCSupplemental.

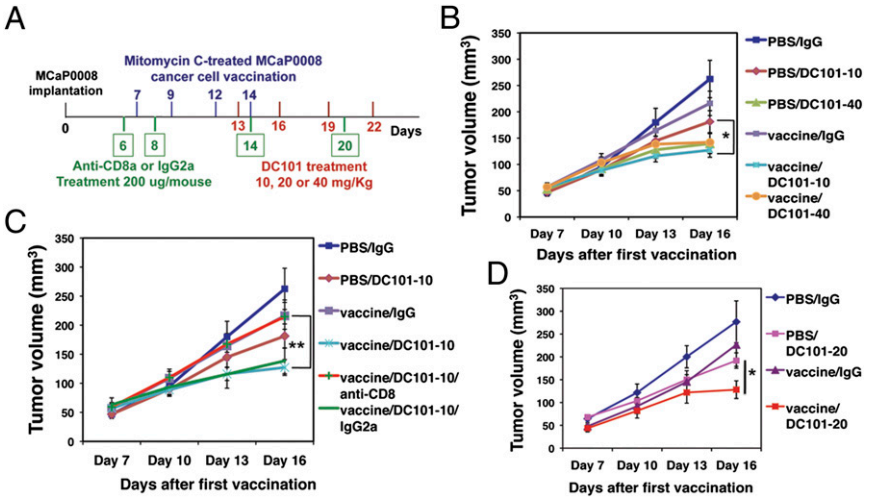

Fig. 1. Lower-dose DC101 treatment enhances vaccine therapy in a model of MCaP0008 breast cancer. (*A*) Treatment protocol. Seven days after implantation of an MCaP0008 breast tumor, mice were divided randomly into two groups and injected i.p. with 5×10^6 $CD45^-$, mitomycin C-treated MCaP0008 tumor tissue cells or with an equal volume of PBS at four time points. These mice subsequently were treated with four doses of DC101 [10 or 40 mg/kg body weight (bw)] at 3-d intervals or with IgG (40 mg/kg bw) 1 d before the fourth vaccination. Mice in the in vivo CD8 depletion study were treated with anti-CD8a or 2A3 (isotype rat IgG2a, 200 μg per mouse) on days −1 (1 d before the first vaccination), 1, 7, and 13. (*B*) Tumor growth curves. Tumor size was measured every 3 d starting at day 7 after the first vaccination (the first day of DC101 treatment). $*P < 0.05$, PBS/DC101-10 vs. vaccine/DC101-10. $n = 10$ mice per group. (*C*) Depletion of CD8 T-cells abrogated the improvement of quarter-dose DC101 treatment on vaccine therapy. $**P < 0.01$,vaccine/DC101-10 vs. vaccine/DC101-10/anti-CD8. The IgG2a group had six mice; all other groups had 10 mice. (*D*) Tumor growth curves. MCaP0008 tumor-bearing mice were treated with rat IgG, half-dose DC101, vaccine, or a combination as described in *A*. Tumor size was measured at 3-d intervals. $*P < 0.05$. $n = 8$–11 mice per group. Data are mean ± SEM.

lated IFN-γ production in splenic $CD8^+$ T cells (Fig. S1), vaccination alone did not inhibit tumor growth, suggesting the immune tolerance of MCaP0008 breast cancer (Fig. 1*B*). Consistent with previous preclinical studies (26), monotherapy with a standard antivascular/antiangiogenic high-dose DC101 (40 mg/kg, hereafter referred as "full-dose"), but not lower-dose DC101 (10 mg/kg, hereafter referred to as "quarter-dose"), significantly delayed tumor growth (Fig. 1*B*). However, the combination of full-dose DC101 and vaccine treatment did not show any further inhibition of tumor growth compared with full-dose DC101 monotherapy. Remarkably, tumor growth was inhibited significantly by quarter-dose DC101 combined with vaccine treatment as compared with quarter-dose DC101 alone ($P = 0.038$) (Fig. 1*B*). In vivo depletion of $CD8^+$ T cells abrogated the improvement seen with the combination of quarter-dose DC101 and vaccine treatment, indicating that quarter-dose DC101 treatment improved vaccine therapy in a $CD8^+$ T-cell–dependent manner (Fig. 1*C*). Similarly, the combination of half-dose DC101 (20 mg/kg) and vaccine therapy significantly reduced tumor volume as compared with half-dose DC101 monotherapy ($P = 0.031$) (Fig. 1*D*). These data show that lower-, but not high-dose, anti-VEGFR2 antibody treatment enhances the anticancer efficacy of a vaccine therapy in a model of immune-tolerant breast cancer.

Lower-Dose Anti-VEGFR2 Antibody Treatment Normalizes Breast Tumor Vasculature and Improves Overall Tissue Perfusion. Abnormal tumor vasculature and the immunosuppressive tumor microenvironment are two major barriers for cancer vaccine therapy (6, 8, 9, 16). We hypothesized that lower-dose antiangiogenic treatment, in contrast to a high dose, alleviates the immunosuppressive tumor microenvironment via vascular normalization. Here, we adapted a previously established procedure to label tumor areas proximal to perfused vessels with Hoechst 33342. Thus, Hoechst fluorescence positivity is inversely related to hypoxia status (27). We analyzed perfusion in entire cross-sections of tumor tissue using confocal image mosaic and computer-assisted image analysis (Fig. 2*A*). Quantitative analysis revealed that a significantly higher fraction of the tissue area was perfused in tumors treated with half- and quarter-dose, but not full-dose, DC101 as compared with IgG control (Fig. 2*B*). Consistently, quarter-dose DC101 treatment significantly reduced the hypoxic area as compared with both IgG control and full-dose DC101 treatment (Fig. 2*C* and Fig. S2*C*). In addition, we found a remarkable change in the distribution of perfused tumor vessels between control tumors and tumors treated with low-dose DC101. In IgG control tumors, perfused vessels were distributed unevenly throughout the tumor. Some areas of tumor tissue were well perfused, but other areas had little or no perfusion (Fig. 2 *A* and *D*). In contrast, with quarter- and half-dose DC101 treatments, perfused vessels were distributed more evenly throughout the tumor section. [The variances are significantly different in IgG vs. quarter-dose ($P = 0.027$) and IgG vs. half-dose ($P = 0.026$), exact Wilcoxon test; areas under relative operating characteristic (ROC) curves are 0.76 and 0.77, respectively (Fig. 2 *A* and *D*).] On the other hand, there was no significant improvement in functional vessel distribution with full-dose DC101 treatment (Fig. 2 *A* and *D*). These data indicate that only lower-dose DC101 treatment results in a more homogeneous distribution of functional blood vessels in tumors.

To dissect further the mechanisms of improved tumor perfusion during lower-dose DC101 treatment, we evaluated pericyte coverage (a measure of vessel maturation) using NG2 immunostaining and tumor vessel perfusion by labeling functional vessels with i.v.-injected FITC-lectin. Consistently, half-dose DC101 treatment significantly increased NG2-positive pericyte coverage (Fig. 2*E*) and the proportion of functional vessels labeled by FITC-lectin in comparison with IgG control (Fig. 2*F*). Together, these data demonstrate that lower-dose DC101 treatment normalizes breast tumor vasculature and improves tissue distribution of functional blood vessels in breast cancers.

Lower-Dose Anti-VEGFR2 Antibody Treatment Polarizes the Number, Distribution, and Phenotype of Tumor-Infiltrating Myeloid Cells from Immunosuppressive to Immunostimulatory. In breast cancer, the abundant TAMs and MDSCs suppress anticancer immunity and promote tumor progression (5, 8, 14, 16). Considering the positive effects of lower-dose DC101 on vaccine therapy, we determined whether lower-dose DC101 treatment could modulate the tumor infiltration, distribution, and phenotype of immune-suppressive myeloid cells. We found that lower-dose, but not full-dose, DC101 treatment significantly reduced the fraction of $CD45^+CD11b^+Gr1^+F4/80^-$ cells ($CD11b^+Gr1^+$ or MDSC) in total viable cells in MCaP0008 breast cancer tissues (Fig. 3*A* and Fig. S3*A*). Concurrently, lower-dose DC101 treatment significantly increased the percentage of $CD45^+CD11b^+Gr1^-F4/80^+$ TAMs in total viable cells as compared with IgG control or full-dose DC101 treatment (Fig. 3*A* and Fig. S3*A*). To differentiate TAMs proximal and distal to blood vessels, we injected Hoechst 33342 dye i.v. before tissue harvest. TAMs were separated by flow cytometry as Hoechst 33342-positive TAMs (Ho^+TAMs) proximal to perfused vessels and Hoechst 33342-negative TAMs (Ho^-TAMs) distal to perfused vessels. We found that full-dose DC101 treatment significantly decreased the percentage of Ho^+TAMs among total TAMs in

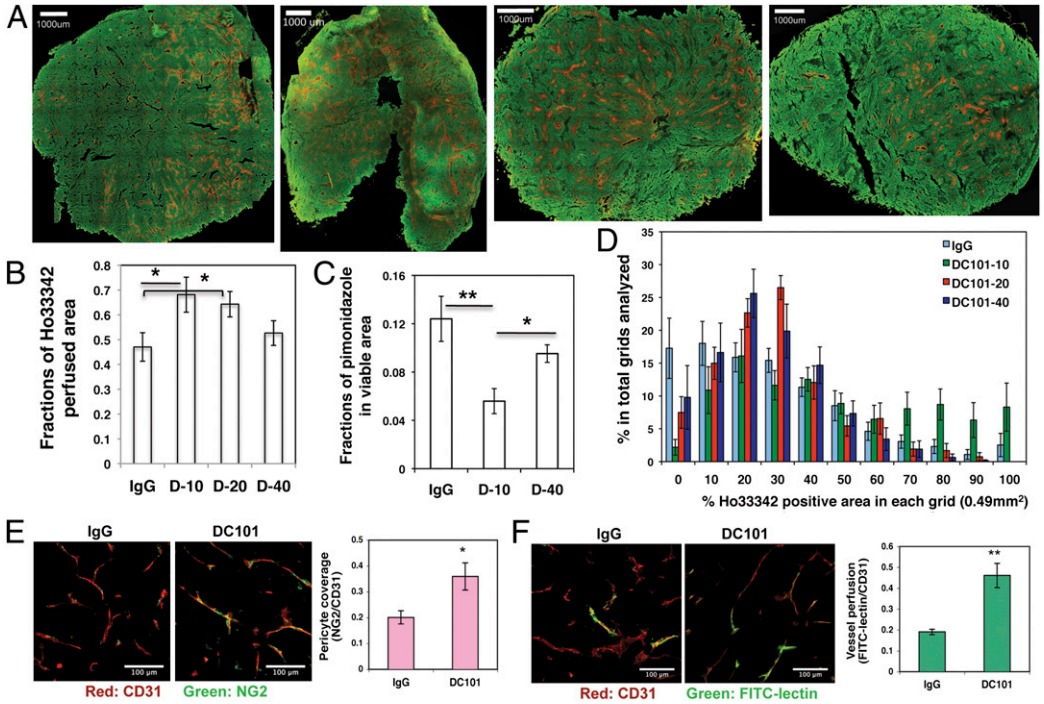

Fig. 2. Lower-dose DC101 treatment normalizes breast tumor vasculature. When MCaP0008 tumors reached 4–5 mm in diameter, mice were treated with four doses of DC101 (10, 20, or 40 mg/kg bw) or rat IgG (40 mg/kg bw) as control administered at 3-d intervals. Mice were injected i.v. with 200 μg Hoechst 33342 before tumor harvest on day 11 after DC101 treatment. Perfusion images of whole tumor tissue were taken by multispectral confocal microscopy. (*A*) Representative perfusion images of whole tumor tissue treated with (*Left* to *Right*) IgG, DC101-10, DC101-20, and DC101-40. Green, Sytox staining; red, Hoechst 33342 staining. (Scale bars, 1,000 μm.) (*B*) The fractions of Hoechst 33342-positive area in whole tumor area. $n = 10$–14 mice per group. $^*P < 0.05$. (*C*) The fractions of pimonidazole-positive area in total viable areas. $n = 10$ mice per group. $^*P < 0.05$, $^{**}P < 0.01$. (*D*) A distribution histogram of the Ho33342-positive areas. Tumor areas were subdivided based on a 700-μm grid, the percentage of Hoechst 33342-positive area in each grid was quantified, and their fractions in the total grid were calculated for each tumor. A distribution histogram for each group was plotted. The *x*-axis shows the percentage of Ho33342-positive area in each grid (0.49 mm^2). The *y*-axis shows the percentage of Ho33342-positive area in the total grids analyzed. $n = 10$–14 mice per group. (*E*) Quantification of pericyte coverage (fraction of area covered) in DC101- and IgG-treated groups (20 mg/kg). CD31-positive endothelial cells are stained red; NG2-positive pericytes are stained green. Confocal images were taken within randomly selected fields excluding the tumor periphery (four to six fields per tumor, six to eight tumors per group). A 20× objective was used for imaging. (Scale bars, 100 μm.) (*F*) Quantification of tumor vessel perfusion (fraction of area perfused) in DC101- and IgG-treated groups (20 mg/kg). CD31-positive endothelial cells are stained red; FITC-lectin–perfused vessels are stained green. Data are shown as mean ± SEM. $^{**}P < 0.01$.

MCaP0008 breast tumors as compared with IgG control and lower-dose DC101 treatments (Fig. 3*B* and Fig. S3*B*).

Next, we tested the effect of DC101 treatment on a spontaneous MMTV-PyVT breast cancer, a widely used mouse model of breast cancer that recapitulates the progression of breast cancer in humans (28). We orthotopically transplanted spontaneous MMTV-PyVT breast tumors into syngeneic FVB mice and treated these mice bearing first-generation (F1) isografts with IgG or DC101. We confirmed that full-dose DC101 treatment significantly decreased Ho^+TAMs in MMTV-PyVT breast tumors compared with IgG control and quarter-dose DC101 treatment (Fig. 3*C* and Fig. S3*C*). Together, our data suggest that lower-dose DC101 treatment decreases $CD11b^+Gr1^+$ cells, whereas high-dose DC101 treatment decreases a subset of TAMs proximal to perfused tumor vessels in murine breast cancer models.

The abnormal tumor vasculature creates a highly heterogeneous and hypoxic tumor microenvironment (4) that can convert TAMs to an immune-suppressive M2-like phenotype (14, 17, 18). Thus, we hypothesized that TAMs in the area distal to perfused vessels have more M2-like features than TAMs proximal to perfused vessels. Indeed, flow-sorted Ho^-TAMs had expressed higher levels of M2-like genes, including *Arg1*, *CSF-1*, *TGF-β*, and *MMP9*, as compared with Ho^+TAMs (Fig. S4*A*). Next, we examined whether lower-dose DC101 treatment polarizes TAMs to an immunosupportive M1-like phenotype to facilitate a vaccine therapy. Indeed, lower-dose DC101 treatments (10 and 20 mg/kg) up-regulated

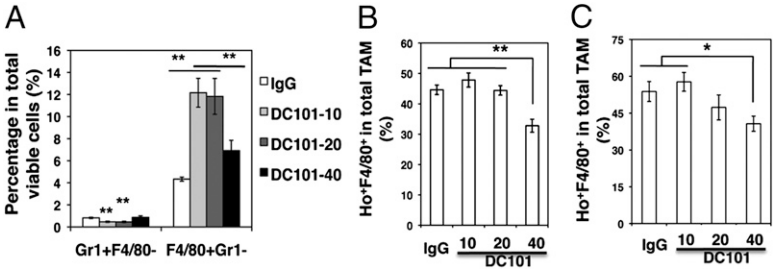

Fig. 3. Lower-dose DC101 treatment decreases $CD11b^+Gr1^+$ cells, whereas high-dose DC101 treatment decreases the proportion of TAMs proximal to perfused tumor vessels. When tumors reached 4–5 mm in diameter, MCaP0008 or MMTV-PyVT tumor-bearing mice were treated with DC101 or IgG. Tumors were perfused with Hoechst 33342 as described in Fig 2 and then were harvested. (*A*) Percentages of $CD11b^+Gr1^+$ and TAM cells in total viable cells in MCaP0008 tumors. (*B*) Full-dose DC101 treatment decreased the proportion of Ho^+TAMs in total TAMs in MCaP0008 tumors. (*C*) Full-dose DC101 treatment decreased the proportion of Ho^+TAMs in total TAMs in MMTV-PyVT tumors. Data are shown as mean ± SEM. $n = 8$–10 mice per group in *A* and *B*; $n = 5$ mice per group in *C*. $^*P < 0.05$, $^{**}P < 0.01$.

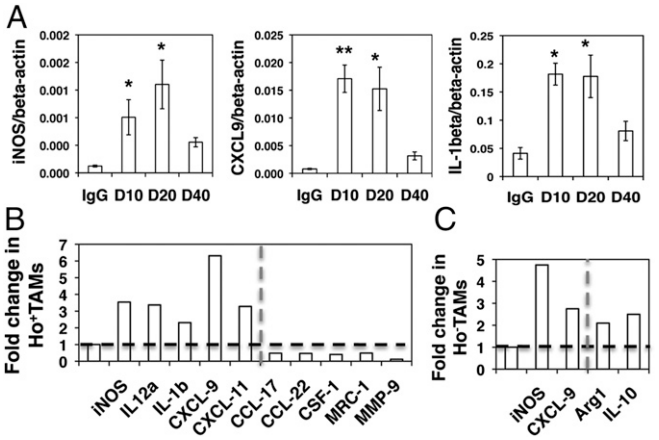

Fig. 4. Lower-dose DC101 treatment polarizes perivascular TAMs to an M1-like phenotype. MCaP0008 tumor-bearing mice were treated with DC101 (10, 20, or 40 mg/kg bw) or IgG (40 mg/kg bw) and were perfused with Hoechst33342 as described in Fig. 2. Gene transcription in different TAM populations was analyzed by quantitative real-time PCR (Table S1). (*A*) In MCaP0008 tumors lower-dose (10 and 20 mg/kg bw) DC101 treatments up-regulated typical M1-like gene expression in TAMs as compared with both IgG and full-dose (40 mg/kg bw) DC101 treatment. TAMs were enriched by CD11b-microbead and separated by flow sorting. $*P < 0.05$, $**P < 0.01$. (*B*) Half-dose DC101 treatment elevated expression of M1-like genes and down-regulated expression of M2-like genes in Ho^+TAMs. (*C*) Ho^-TAMs displayed a mixed M1/M2-like phenotype after half-dose DC101 treatment. Data are shown as mean ± SEM. TAMs from 8–10 tumors were pooled as three samples in each group. (*B* and *C*) Horizontal dash: the value of 1. Vertical dash: separates the genes as M1-type (left side) and M2-type (right side).

M1-like gene transcription compared with full-dose DC101 (Fig. 4*A*). We separated Ho^+TAMs and Ho^-TAMs and analyzed their phenotypes. Remarkably, in Ho^+TAMs half-dose DC101 treatment significantly elevated the levels of M1-type genes (*iNOS*, *IL-12a*, *IL-β*, *CXCL-9*, and *CXCL-11*) and reduced the expression of M2-type genes (*CCL-17*, *CCL-22*, *CSF-1*, and *MMP9*) as compared with IgG control (Fig. 4*B*). Consistently, quarter-dose DC101 treatment substantially elevated *iNOS* and *IL-12a* and decreased *Arg1* compared with IgG control and full-dose DC101 treatment in MMTV-PyVT tumors (Fig. S4*B*). Ho^-TAMs displayed mixed M1/M2-like phenotypes after half-dose DC101 treatment: In MCaP0008 tumors they had elevated levels of both typical M1 markers (*iNOS* and *CXCL-9*) and M2-markers (*Arg1* and *IL-10*), as compared with IgG control (Fig. 4*C*). However, full-dose DC101 treatment did not redirect TAMs to an M1-like phenotype in either breast cancer model (Fig. 4*A* and Fig. S4*B*). In summary, these data indicate that lower-dose DC101 treatment changes the number and distribution of tumor-infiltrating myeloid cells and polarizes TAM from an immunosuppressive to an immunostimulatory phenotype.

Lower-Dose Anti-VEGFR2 Antibody Treatment Promotes T-Cell Tumor Infiltration More Potently than Full-Dose Treatment. Improvement of tumor vascular function and polarization of TAMs to an M1-like phenotype can facilitate T-cell tumor infiltration (9, 14, 17). Thus, we evaluated the effect of various doses of DC101 treatment on T-cell infiltration into tumors. In MCaP0008 tumors, flow cytometric analysis revealed significantly increased tumor-infiltrating $CD4^+$ and $CD8^+$ T cells in all DC101-treated groups (10–40 mg/kg) compared with IgG control (Fig. 5*A* and Fig. S5). Interestingly, the increase in T-cell tumor infiltration appeared inversely correlated with DC101 doses. Quarter-dose DC101 treatment significantly increased the percentage of tumor-infiltrating $CD8^+$ T cells compared with full-dose DC101 treatment (Fig. 5*A*). Furthermore, the proportion of Hoechst 33342^+CD8^+ T cells was higher after quarter-dose DC101 treatment than after either IgG control or full-dose DC101 treatment (Fig. 5*B*). To validate this finding further, we treated F1 isografts of spontaneous MMTV-PyVT breast cancer with IgG or DC101 at different doses (10, 20, and 40 mg/kg). Only quarter-dose DC101 treatment significantly increased tumor-infiltrating $CD4^+$ and $CD8^+$ T cells (Fig. 5 *C* and *D*) compared with IgG control. In addition, we tested a spontaneous autochthonous breast cancer in syngeneic C3H mice by transplanting it orthotopically in C3H mice. Consistently, half-dose DC101 treatment increased tumor-infiltrating $CD8^+$ T cells as compared with full-dose DC101 treatment or IgG control (Fig. S6). Together, these data demonstrate that lower-dose DC101 is more effective than high-dose treatment in facilitating $CD8^+$ T-cell tumor infiltration in breast cancers.

Lower-Dose Anti-VEGFR2 Antibody Combined with Vaccine Prolongs Survival in a Model of MMTV-PyVT Breast Cancer. Next, we tested the dose effect of anti-VEGFR2 antibody treatment on cancer vaccine therapy in a model of immunogenic MMTV-PyVT breast cancer. Whole cancer tissue cell vaccination alone induced regression of MMTV-PyVT breast cancer, supporting its immunogenic character (Fig. 6*A*). Consistent with the inhibition of tumor growth, vaccination dramatically increased tumor-infiltrating $CD8^+$ T cells, up-regulated IFN-γ expression in CD8 T cells, and reduced the proportion of tumor-infiltrating $CD4^+CD25^+FoxP3^+$ Tregs within the $CD4^+$ T-cell population (Fig. 6 *B* and *C* and Fig. S7). These data demonstrated that the whole cancer tissue cell vaccine induced a potent anticancer immune response. Quarter-dose DC101 treatment appeared to stabilize tumor growth, whereas full-dose DC101 induced tumor regression (Fig. 6*A*). Together, these data indicated that orthotopically transplanted MMTV-PyVT breast cancers are immunogenic and very sensitive to DC101 treatment. In this setting, both 10- and 40-mg/kg DC101 treatments combined with vaccine moderately enhanced the inhibition of tumor growth during the treatment period, as compared with vaccine alone (Fig. 6*A*). Interestingly, after termination of treatment, the combination of quarter-dose DC101 and vaccine therapy resulted in a significant prolongation of survival as compared with vaccine monotherapy

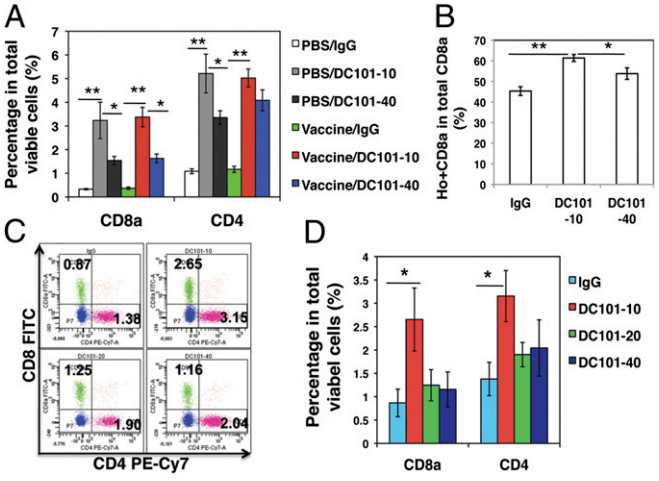

Fig. 5. Lower-dose DC101 treatment promotes the infiltration of T cells into breast cancer parenchyma. MCaP0008 (*A* and *B*) and MMTV-PyVT (*C* and *D*) tumor-bearing mice were treated with DC101 or rat IgG as described in Figs. 2 and 3. (*A*) Percentage of $CD4^+$ and $CD8^+$ T cells in total viable cells. $n = 10$ mice per group. In $7AAD^-CD45^+$ tumor-infiltrating immune cells, lymphoid cells were gated according to the side scatter (SSC) and forward scatter (FSC) and were analyzed for expression of CD4 and CD8a by flow cytometry. $*P < 0.05$, $**P < 0.01$. (*B*) Quarter-dose DC101 treatment increased the proportion of Hoechst 33342-positive $CD8^+$ (Ho^+CD8^+) T cells in total $CD8^+$ T cells in MCaP0008 tumors. $n = 10$ mice per group. $*P < 0.05$, $**P < 0.01$. (*C*) Representative flow figures of tumor-infiltrating $CD4^+$ and $CD8^+$ T cells in spontaneous MMTV-PyVT breast tumors. Numbers show the percentages of $CD4^+$ and $CD8^+$ T cells in total viable cells. (*D*) The percentage of tumor-infiltrating $CD4^+$ and $CD8^+$ T cells in total viable cells. $n = 5$ mice per group. Data are shown as mean ± SEM. $*P < 0.05$.

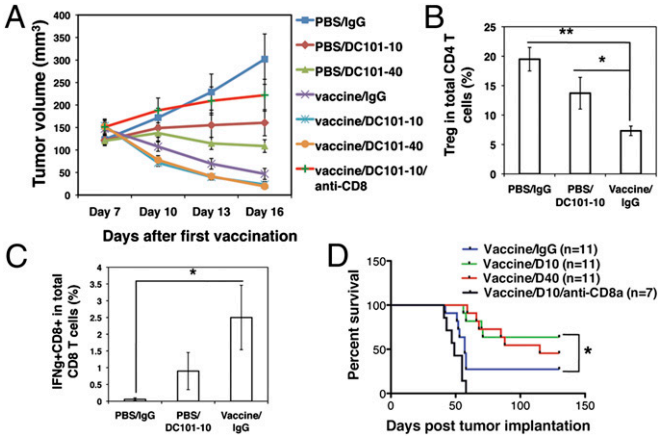

Fig. 6. Quarter-dose DC101 treatment combined with vaccine is sufficient to maximize anticancer efficacy in the MMTV-PyVT tumor model. When orthotopically transplanted MMTV-PyVT tumors reached 3 mm in diameter, mice received vaccine, DC101, IgG, or anti-CD8 antibody treatments as described in Fig 1*A*. (*A*) Tumor growth curves. Tumor size was measured at 3-d intervals beginning on day 7 after the first vaccination (the first day of DC101 treatment). The vaccine/DC101-10/anti-CD8 group had 10 mice; all other groups had 11 mice. (*B*) The percentages of tumor-infiltrating $CD4^+$ $CD25^+Foxp3^+$ Tregs in the total $CD4^+$ T-cell population. $n = 8$ mice per group. $^*P < 0.05$, $^{**}P < 0.01$. (*C*) Vaccination up-regulated IFN-γ production in MMTV-PyVT tumors. Mitomycin C-treated whole breast tumor tissue cells were used for vaccination. Tumor-infiltrating $CD8^+$ T cells were isolated by anti-CD8 microbeads and then were stimulated by coculturing with mitomycin C-treated whole tumor cells in vitro. $IFN\gamma^+CD8^+$ T cells were analyzed by flow cytometry. $n = 8$ mice per group. $^*P < 0.05$. (*D*) The combination of quarter-dose DC101 treatment and vaccine improved survival significantly compared with vaccine monotherapy. Mice were euthanized when tumors reached 1,300 mm^3. $P < 0.0001$, vaccine/DC101-10 vs. vaccine/DC101-10/anti-CD8; $P < 0.05$, vaccine/IgG vs. vaccine/DC101-10 (log-rank test). The vaccine/DC101-10/anti-CD8 group had seven mice; all other groups had 11 mice. Data are shown as mean ± SEM. $^*P < 0.05$.

($P < 0.05$, vaccine/IgG vs. vaccine/DC101-10; $P = 0.07$, vaccine/IgG vs. vaccine/DC101-40; log-rank test) (Fig. 6*D*). Depletion of $CD8^+$ T cells in vivo significantly shortened the survival, demonstrating that the improvement in survival is $CD8^+$ T-cell–dependent in the vaccine plus quarter-dose DC101 group (Fig. 6*D* and Fig. S8). Collectively, these data suggest that lower-dose anti-VEGFR2 antibody treatment is sufficient to maximize the anticancer efficacy when combined with a vaccine therapy in a model of immunogenic breast cancer sensitive to both vaccine and antiangiogenic therapies and that $CD8^+$ T cells mediate this effect.

Discussion

Malignant tumors escape from host immune surveillance through multiple mechanisms (5, 7–9). Of these, abnormal tumor vasculature and numerous immune-inhibitory factors produced by tumor-infiltrating myeloid cells are critical in establishing an immunosuppressive tumor microenvironment and, consequently, impeding active cancer immunotherapy. Our study demonstrates that lower-dose antiangiogenic treatment normalizes tumor vasculature, polarizes TAMs to reduce immune-regulatory signals, and thereby creates an immune-supportive microenvironment to recruit and activate $CD8^+$ T cells. Through this mechanism, lower-dose antiangiogenic treatment enhances the anticancer efficacy of a vaccine therapy. In contrast, high-dose antiangiogenic/antivascular treatment has smaller or adverse effects on the tumor immune microenvironment (Fig. 7).

Antiangiogenic treatment is an established therapy in several solid cancers (29). Although bevacizumab alone does not improve clinical outcome, the combination of bevacizumab with chemotherapy prolongs the survival of patients with advanced non-small cell lung cancer and metastatic colorectal cancer (29–31). However, the clinical benefits are in the order of months, and resistance eventually develops (29). The role of antiangiogenic therapy in breast cancer remains controversial. Addition of bevacizumab to chemotherapy improved progression-free survival in patients with advanced breast cancer but resulted in no overall survival benefit in three large randomized phase III trials (32–34). These disappointing results raise questions about how antiangiogenic therapy might be used more effectively in treating cancer, especially breast cancer.

Antiangiogenic agents generally are used at relatively high doses [bevacizumab, 10 or 15 mg/kg body weight (bw)] to treat breast cancers (32, 33). It is likely that high-dose antiangiogenic therapy prunes tumor vessels excessively, rather than normalizing them, and thus decreases the delivery of chemotherapeutics (31, 33, 35). This excessive pruning also may exacerbate, rather than reverse, the immunosuppressive tumor microenvironment and thus may compromise the efficacy of active cancer immunotherapy. In this study, we showed that lower-dose DC101 treatment did not change vessel density in tumors significantly (Fig. S2) but normalized tumor vessels by improving overall vessel perfusion and creating a homogeneous distribution of perfused vessels throughout the tumor. As a result more T cells can be delivered into tumors (9, 36). Improved vessel perfusion and decreased hypoxia could polarize TAMs to an M1-like phenotype, and, in turn, elevated CXCL9 expression in M1-like TAMs further promotes T-cell tumor infiltration (14). In addition, low-dose DC101 treatment increased TAMs and decreased MDSCs in MCaP0008 tumors. This effect might be caused by the promotion of differentiation of MDSCs toward M1-like TAMs by low-dose DC101 (16). Furthermore, lower-dose antiangiogenic therapy is likely to reduce toxicity as well as drug resistance. Therefore, our study suggests that appropriate lower-dose antiangiogenic therapy could be an effective strategy to reengineer the tumor microenvironment for active immunotherapies in a clinical setting.

Different breast cancers have different immunogenicity and respond differently to a cancer vaccine therapy. In immunogenic MMTV-PyVT breast cancers, vaccination alone dramatically increased $CD8^+$ T cells in tumor tissue and led to tumor regression. However, in immune-tolerant MCaP0008 breast cancers, vaccination alone did not increase $CD8^+$ T-cell tumor infiltration and did not inhibit tumor growth, even though vaccination activated $CD8^+$ T cells in the spleen. When we compare the intratumor vessels in these cancer models, the vasculature in MMTV-PyVT

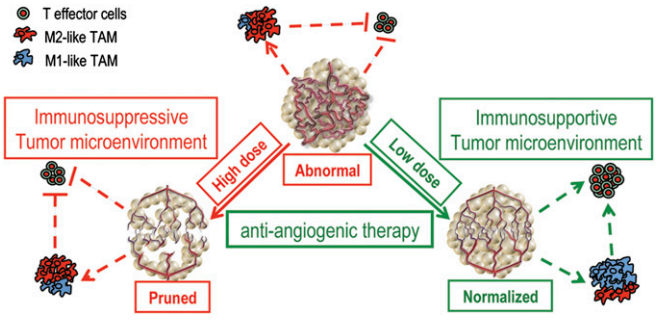

Fig. 7. A schematic model showing that lower-dose DC101 treatment reprograms the tumor microenvironment from immunosuppressive to immunosupportive and potentiates cancer vaccine therapy. Abnormal tumor vasculature creates a hypoxic tumor microenvironment, which impedes the infiltration of T effector cells into the tumor and polarizes TAMs to the immune-inhibitory M2-like phenotype that suppresses the function of T effector cells. Lower-dose antiangiogenic treatment normalizes the tumor vasculature and generates a homogeneous distribution of perfused tumor vessels, which promotes the infiltration of T effector cells, redirects TAMs to an immune stimulatory M1-like phenotype, and thereby substantially improves the anticancer efficacy of a cancer vaccine therapy. Conversely, high-dose antiangiogenic treatment prunes tumor vessels, increases hypoxia, fails to induce TAM M1-like polarization, and restricts the infiltration of T effector cells into tumor parenchyma, resulting in impaired cancer vaccine therapy.

cancer appears to be more functional than that in MCaP0008 cancer in term of pericyte coverage and vessel perfusion (Fig. 2 *E* and *F* and Fig. S9). These factors may be favorable for the infiltration of activated $CD8^+$ T cells and elicit a relatively immunosupportive tumor microenvironment.

Vaccine therapy usually requires time to generate, activate, and boost a host immune response against a tumor. Vaccination of MMTV-PyVT cancer cells pretreated with mitomycin C appeared to induce tumor regression 10 d after vaccination. Our previous reports indicated that antiangiogenic treatment could normalize tumor vessels as early as 2 d posttreatment (4, 19). Therefore, the schedule of combination treatment (Fig. 1*A*) was designed to synchronize vascular normalization and T-cell activation. A previous study suggested that antiangiogenic therapy preceding vaccine therapy had a better anticancer effect than vaccine therapy followed by antiangiogenic treatment (37). Thus, a comparison of the efficacy of different combination schedules might yield even better treatment regimens in the future.

In summary, our data provide preclinical evidence that lower-dose antiangiogenic therapy can normalize breast tumor vasculature, reprogram the tumor microenvironment from immunosuppressive to immunosupportive, and enhance a cancer vaccine therapy (Fig. 7). This finding may have implications beyond active immunotherapy in breast cancer, where the use of low doses of bevacizumab with chemotherapy ultimately may contribute to improvements of overall survival (33, 34).

Materials and Methods

Fragments of spontaneous murine mammary carcinoma from *MMTV-PyVT* mice or MCaP0008 tumor fragments (38) were implanted orthotopically in the mammary fat pad of syngeneic immunocompetent FVB mice. When tumors reached 4–5 mm in diameter, mice were divided into appropriate groups and received four doses by i.p. injection of either control rat IgG or DC101 (10, 20, or 40 mg/kg bw) administered at 3-d intervals. For vaccination experiments, breast tumor-bearing mice were divided randomly into appropriate groups and received four i.p. injections of 5×10^6 mitomycin C-treated, $CD45^-$ breast tumor tissue cells or an equal volume of PBS, administered at 2- to 3-d intervals (Fig. 1*A*). CD8 T cells were depleted using 200 μg anti-CD8a monoclonal antibody. On the day before the last vaccination, both vaccination and control groups were divided randomly into several groups and were treated with different doses of DC101 or IgG. Experimental procedures are explained in detail in *SI Materials and Methods*.

ACKNOWLEDGMENTS. We thank ImClone/Lilly for their gift of DC101; Glenn Dranoff for advice on cancer vaccine preparation; Sylvie Roberge, Julia Kahn, Carolyn Smith, Ned Kirkpatrick, Ramone Williams, Madzia Kowalski, Rachel Ingraham, and Amy Yang for technical assistance; and Shom Goel, Vikash Chauhan, Eleanor Ager, and Sergey Kozin for their helpful scientific input. This work was supported by National Institutes of Health Grants R01-CA115767 and R01-CA126642 (to R.K.J.), R01-CA096915 (to D.F.), and R21-CA139168 and R01-CA159258 (to D.G.D.); a National Cancer Institutes Federal Share grant (to M.C.P. and J.Y.); Department of Defense (DoD) Breast Cancer Innovator Award W81XWH-10-1-0016 (to R.K.J.); DoD Research Fellowship W81XWH-11-1-0619 (to Y.H.). This work was also supported by the Marsha Rivkin Foundation (E.R. and M.C.P.), Friends of the Vaccine and Immunotherapy Center, and the Frank Lynch Jr. Cancer Research Fund (J.Y. and M.C.P.).

1. Madan RA, Gulley JL, Fojo T, Dahut WL (2010) Therapeutic cancer vaccines in prostate cancer: The paradox of improved survival without changes in time to progression. *Oncologist* 15:969–975.
2. Rosenberg SA, et al. (2005) Tumor progression can occur despite the induction of very high levels of self/tumor antigen-specific CD8+ T cells in patients with melanoma. *J Immunol* 175:6169–6176.
3. Offringa R (2006) Cancer. Cancer immunotherapy is more than a numbers game. *Science* 314:68–69.
4. Jain RK (2005) Normalization of tumor vasculature: An emerging concept in antiangiogenic therapy. *Science* 307:58–62.
5. Schmid MC, Varner JA (2010) Myeloid cells in the tumor microenvironment: Modulation of tumor angiogenesis and tumor inflammation. *J Oncol* 2010:201026.
6. DeNardo DG, et al. (2011) Leukocyte complexity predicts breast cancer survival and functionally regulates response to chemotherapy. *Cancer Discov* 1(1):54–67.
7. Quezada SA, Peggs KS, Simpson TR, Allison JP (2011) Shifting the equilibrium in cancer immunoediting: From tumor tolerance to eradication. *Immunol Rev* 241: 104–118.
8. Schlom J (2012) Therapeutic cancer vaccines: Current status and moving forward. *J Natl Cancer Inst* 104:599–613.
9. Hamzah J, et al. (2008) Vascular normalization in Rgs5-deficient tumours promotes immune destruction. *Nature* 453:410–414.
10. Huang Y, et al. (2007) Distinct roles of VEGFR-1 and VEGFR-2 in the aberrant hematopoiesis associated with elevated levels of VEGF. *Blood* 110:624–631.
11. Wu NZ, Klitzman B, Dodge R, Dewhirst MW (1992) Diminished leukocyte-endothelium interaction in tumor microvessels. *Cancer Res* 52:4265–4268.
12. Jochems C, Schlom J (2011) Tumor-infiltrating immune cells and prognosis: The potential link between conventional cancer therapy and immunity. *Exp Biol Med (Maywood)* 236:567–579.
13. Liyanage UK, et al. (2002) Prevalence of regulatory T cells is increased in peripheral blood and tumor microenvironment of patients with pancreas or breast adenocarcinoma. *J Immunol* 169:2756–2761.
14. Biswas SK, Mantovani A (2010) Macrophage plasticity and interaction with lymphocyte subsets: Cancer as a paradigm. *Nat Immunol* 11:889–896.
15. Schmid MC, et al. (2011) Receptor tyrosine kinases and TLR/IL1Rs unexpectedly activate myeloid cell PI3kγ, a single convergent point promoting tumor inflammation and progression. *Cancer Cell* 19:715–727.
16. Corzo CA, et al. (2010) HIF-1α regulates function and differentiation of myeloid-derived suppressor cells in the tumor microenvironment. *J Exp Med* 207:2439–2453.
17. Rolny C, et al. (2011) HRG inhibits tumor growth and metastasis by inducing macrophage polarization and vessel normalization through downregulation of PlGF. *Cancer Cell* 19:31–44.
18. Huang Y, Snuderl M, Jain RK (2011) Polarization of tumor-associated macrophages: A novel strategy for vascular normalization and antitumor immunity. *Cancer Cell* 19: 1–2.
19. Winkler F, et al. (2004) Kinetics of vascular normalization by VEGFR2 blockade governs brain tumor response to radiation: Role of oxygenation, angiopoietin-1, and matrix metalloproteinases. *Cancer Cell* 6:553–563.
20. Chauhan VP, et al. (2012) Normalization of tumour blood vessels improves the delivery of nanomedicines in a size-dependent manner. *Nat Nanotechnol* 7:383–388.
21. Sorensen AG, et al. (2012) Increased survival of glioblastoma patients who respond to antiangiogenic therapy with elevated blood perfusion. *Cancer Res* 72:402–407.
22. Li B, et al. (2006) Vascular endothelial growth factor blockade reduces intratumoral regulatory T cells and enhances the efficacy of a GM-CSF-secreting cancer immunotherapy. *Clin Cancer Res* 12:6808–6816.
23. Manning EA, et al. (2007) A vascular endothelial growth factor receptor-2 inhibitor enhances antitumor immunity through an immune-based mechanism. *Clin Cancer Res* 13:3951–3959.
24. Shrimali RK, et al. (2010) Antiangiogenic agents can increase lymphocyte infiltration into tumor and enhance the effectiveness of adoptive immunotherapy of cancer. *Cancer Res* 70:6171–6180.
25. Righi E, et al. (2011) CXCL12/CXCR4 blockade induces multimodal antitumor effects that prolong survival in an immunocompetent mouse model of ovarian cancer. *Cancer Res* 71:5522–5534.
26. Prewett M, et al. (1999) Antivascular endothelial growth factor receptor (fetal liver kinase 1) monoclonal antibody inhibits tumor angiogenesis and growth of several mouse and human tumors. *Cancer Res* 59:5209–5218.
27. Olive PL, Chaplin DJ, Durand RE (1985) Pharmacokinetics, binding and distribution of Hoechst 33342 in spheroids and murine tumours. *Br J Cancer* 52:739–746.
28. Lin EY, et al. (2003) Progression to malignancy in the polyoma middle T oncoprotein mouse breast cancer model provides a reliable model for human diseases. *Am J Pathol* 163:2113–2126.
29. Carmeliet P, Jain RK (2011) Molecular mechanisms and clinical applications of angiogenesis. *Nature* 473:298–307.
30. Hurwitz H, et al. (2004) Bevacizumab plus irinotecan, fluorouracil, and leucovorin for metastatic colorectal cancer. *N Engl J Med* 350:2335–2342.
31. Sandler A, et al. (2006) Paclitaxel-carboplatin alone or with bevacizumab for non-small-cell lung cancer. *N Engl J Med* 355:2542–2550.
32. Miller K, et al. (2007) Paclitaxel plus bevacizumab versus paclitaxel alone for metastatic breast cancer. *N Engl J Med* 357:2666–2676.
33. Robert NJ, et al. (2011) RIBBON-1: Randomized, double-blind, placebo-controlled, phase III trial of chemotherapy with or without bevacizumab for first-line treatment of human epidermal growth factor receptor 2-negative, locally recurrent or metastatic breast cancer. *J Clin Oncol* 29:1252–1260.
34. Miles DW, et al. (2010) Phase III study of bevacizumab plus docetaxel compared with placebo plus docetaxel for the first-line treatment of human epidermal growth factor receptor 2-negative metastatic breast cancer. *J Clin Oncol* 28:3239–3247.
35. Van Cutsem E, Lambrechts D, Prenen H, Jain RK, Carmeliet P (2011) Lessons from the adjuvant bevacizumab trial on colon cancer: What next? *J Clin Oncol* 29:1–4.
36. Johansson A, Hamzah J, Payne CJ, Ganss R (2012) Tumor-targeted TNFα stabilizes tumor vessels and enhances active immunotherapy. *Proc Natl Acad Sci USA* 109: 7841–7846.
37. Farsaci B, Higgins JP, Hodge JW (2012) Consequence of dose scheduling of sunitinib on host immune response elements and vaccine combination therapy. *Int J Cancer* 130:1948–1959.
38. Huang P, Duda DG, Jain RK, Fukumura D (2008) Histopathologic findings and establishment of novel tumor lines from spontaneous tumors in FVB/N mice. *Comp Med* 58:253–263.